Appl. Math. Mech. -Engl. Ed., **39**(2), 153–168 (2018)

Applied Mathematics and Mechanics (English Edition)

https://doi.org/10.1007/s10483-018-2298-6

Weakly nonlinear stability analysis of triple diffusive convection in a Maxwell fluid saturated porous layer*

K. R. RAGHUNATHA[1], I. S. SHIVAKUMARA[1,†], B. M. SHANKAR[2]

1. Department of Mathematics, Bangalore University, Bangalore 560056, India;
2. Department of Mathematics, PES University, Bangalore 560085, India

(Received Jun. 13, 2017 / Revised Aug. 9, 2017)

Abstract The weakly nonlinear stability of the triple diffusive convection in a Maxwell fluid saturated porous layer is investigated. In some cases, disconnected oscillatory neutral curves are found to exist, indicating that three critical thermal Darcy-Rayleigh numbers are required to specify the linear instability criteria. However, another distinguishing feature predicted from that of Newtonian fluids is the impossibility of quasi-periodic bifurcation from the rest state. Besides, the co-dimensional two bifurcation points are located in the Darcy-Prandtl number and the stress relaxation parameter plane. It is observed that the value of the stress relaxation parameter defining the crossover between stationary and oscillatory bifurcations decreases when the Darcy-Prandtl number increases. A cubic Landau equation is derived based on the weakly nonlinear stability analysis. It is found that the bifurcating oscillatory solution is either supercritical or subcritical, depending on the choice of the physical parameters. Heat and mass transfers are estimated in terms of time and area-averaged Nusselt numbers.

Key words Maxwell fluid, triple diffusive convection, nonlinear stability, bifurcation, heat and mass transfer

Chinese Library Classification O175.8, O357.3
2010 Mathematics Subject Classification 76A10, 76E06, 76S05

Nomenclature

d,	depth of the porous layer;	M,	ratio of heat capacities;
Pr_{D},	Darcy-Prandtl number;	t,	time;
$\boldsymbol{g}$,	gravitational acceleration;	p,	pressure;
$\boldsymbol{q}$,	velocity vector;	x, y, z,	space coordinates;
K,	permeability of the porous medium;	α,	horizontal wave number;
$R_{\mathrm{S}i}$,	solute Darcy-Rayleigh number of the ith component;	Λ_1,	stress relaxation parameter;
		α_{T},	thermal expansion coefficient;
$\hat{k}$,	unit vector in the vertical direction;	μ,	dynamic viscosity;
R_{T},	thermal Darcy-Rayleigh number;	$\alpha_{\mathrm{S}i}$,	solute analog of α_{T} $(i=1,2)$;

* Citation: Raghunatha, K. R., Shivakumara, I. S., and Shankar, B. M. Weakly nonlinear stability analysis of triple diffusive convection in a Maxwell fluid saturated porous layer. *Applied Mathematics and Mechanics* (*English Edition*), **39**(2), 153–168 (2018) https://doi.org/10.1007/s10483-018-2298-6

† Corresponding author, E-mail: shivakumarais@bub.ernet.in

ν,	kinematic viscosity;
ϵ,	porosity;
ρ,	fluid density;
κ_{T},	thermal diffusivity;
σ,	growth term;
$\kappa_{\mathrm{S}i}$,	solute diffusivity ($i = 1, 2$);
τ_i,	ratio of diffusivity ($i = 1, 2$);
λ_1,	stress relaxation time;
ψ,	stream function.

Subscripts/superscripts

b,	basic state;
U,	upper boundary;
L,	lower boundary;
$*$,	dimensionless variable.

1 Introduction

The thermal convective instability in a layer of Newtonian fluid-saturated porous media is a classical problem in convective heat transfer, and now it is a well-understood phenomenon. Different effects have been taken into account on this study, and the developments are well documented in the literature[1–4]. The non-Newtonian fluid flows and heat transfer in porous media have been a topic of interest in recent years due to their importance in geophysics, ceramic processing, bioengineering, filtration, liquid composite molding, polymer engineering, and oil reservoir engineering[5–6]. To a large extent, the performance of an oil reservoir depends on the physical nature of the crude oil presented in the reservoir. The light crude oil is essentially Newtonian, but the heavy crude oil is found to exhibit a non-Newtonian fluid behavior. In particular, some oil sand contains waxy crude at shallow depth in reservoirs, which is considered to be a viscoelastic fluid[7–8]. The Darcy-Bénard problem for viscoelastic fluids has received considerable attention in the literature because the study can give necessary information about the mobility control in the oil displacement mechanism, which can improve the efficiency of oil recovery[9–17]. It has been revealed that the convection onset in a viscoelastic fluid-saturated porous medium is oscillatory instead of stationary, which depends on the fluid elasticity. Recently, various types of flow problems for the Oldroyd-B and Maxwell viscoelastic fluids have been analyzed[18–20].

The double diffusive convection in porous media is another interesting topic of research, and has attracted many researchers from various fields of science and engineering due to its wide applications, e.g., the solidification of binary mixtures, the migration of the solutes in water-saturated soils, and the geophysical system, electro-chemistry, and the migration of moisture through the air contained in fibrous insulation. The study reveals a variety of interesting convective phenomena, which are not observed in a single component fluid-saturated porous medium. For example, the exchange principle of stabilities is not always valid, and the conductive base state may become unstable through a growing oscillatory mode. Newtonian fluids have been widely studied on this topic[21–22]. However, the double diffusive convection in a non-Newtonian fluid-saturated porous medium has received only limited attention in the literature[23–25].

Nonetheless, many fluid dynamical systems occurring in nature and engineering applications involve more than two stratifying agencies with different molecular diffusivities, in which a multicomponent convection-diffusion is bound to occur. As a first step towards the understanding of the complex multicomponent convection, Griffiths[26], Pearlstein et al.[27], Straughan and Walker[28], and Straughan and Tracey[29] studied the triple diffusive convection in a fluid layer both experimentally and theoretically. Rudraiah and Vortmeyer[30], Poulikakos[31], and Griffiths[26] studied the counterpart in a layer of porous media. Since the results obtained by these authors were incomplete in the vein of Pearlstein et al.[27], Tracey[32] reconsidered the problem, presented systematically the results similar to those of Pearlstein et al.[27], and performed the nonlinear stability analysis with the energy method. Rionero[33] considered a triply convective diffusive fluid mixture, which saturated a horizontal porous layer. Rionero[34] considered the triple diffusive convection in porous media, obtained the conditions for inhibiting the convective onset, and performed a global nonlinear stability analysis. Ghalambaz et al.[35] theoretically studied the triple diffusive convection in a square porous cavity.

The studies on the triple diffusive convection in porous media are mainly focused on Newtonian fluids, and a corresponding problem for non-Newtonian fluids is in the much-to-be desired state. Although Zhao et al.[36] investigated the triply diffusive convection in a Maxwell fluid-saturated porous layer and obtained the criterion for the onset of stationary and oscillatory convection, their study is silent in revealing some of the unusual behaviors that the system is capable of supporting, which have important implications on the instability of the system. The interest to the present work is of two folds. One is to study the linear instability theory in detail and unveil some remarkable departures from those of single and double diffusive cases. The other is to perform a weakly nonlinear stability analysis to understand the stability of bifurcating the equilibrium solution by deriving a cubic Landau equation. The heat and mass transfer is also discussed in terms of the Nusselt numbers.

2 Mathematical formulation

The physical configuration is shown in Fig. 1. We consider a horizontal layer of an incompressible Maxwell fluid-saturated Darcy porous medium with the thickness d, which contains three stratifying agencies, i.e., the temperature T and two solute concentrations S_i $(i = 1, 2)$. The lower and upper impermeable boundaries of the porous layer are kept at different constant temperatures, T_{L} and T_{U} $(< T_{\mathrm{L}})$, and solute concentrations, $S_{i\mathrm{L}}$ and $S_{i\mathrm{U}}$ $(< S_{i\mathrm{L}})$, respectively, with the sign convention that ΔT $(= T_{\mathrm{L}} - T_{\mathrm{U}}) > 0$ when the temperature is destabilizing and ΔS_i $(= S_{i\mathrm{L}} - S_{i\mathrm{U}}) > 0$ when a solute concentration is stabilizing. A Cartesian coordinate system is chosen such that the z-axis is vertically upwards and the x-axis is horizontal. The gravity is acting vertically downwards with the constant acceleration $\boldsymbol{g} = -g\hat{k}$, where $\hat{k}$ is the unit vector in the vertical direction. The equation of states is given by

$$\rho = \rho_0(1 - \alpha_{\mathrm{T}}(T - T_{\mathrm{L}}) + \alpha_{\mathrm{S1}}(S_1 - S_{1\mathrm{L}}) + \alpha_{\mathrm{S2}}(S_2 - S_{2\mathrm{L}})), \tag{1}$$

where ρ is the fluid density, and ρ_0 is the density at the reference temperature and solute concentration. By analogy with the constitutive equation of the Maxwell fluid, a modified Darcy-Maxwell model is used to describe the flow in a porous medium. The governing nonlinear stability equations in dimensionless form are

$$\Big(1 + \Lambda_1 \frac{\partial}{\partial t}\Big)\Big(\frac{1}{Pr_{\mathrm{D}}}\frac{\partial \boldsymbol{q}}{\partial t} + \nabla p + \Big(- R_{\mathrm{T}}T + R_{\mathrm{S1}}S_1 + R_{\mathrm{S2}}S_2\Big)\hat{k}\Big) = -\boldsymbol{q}, \tag{2}$$

$$A\frac{\partial T}{\partial t} + (\boldsymbol{q} \cdot \nabla)T = \nabla^2 T, \tag{3}$$

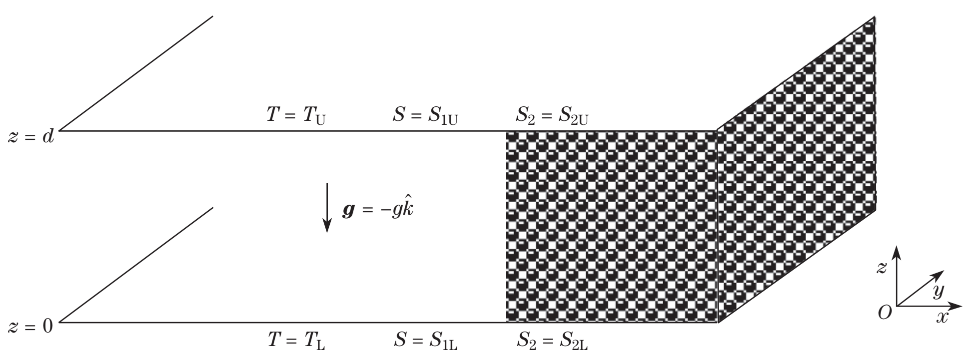

Fig. 1 Physical configuration

$$\frac{\partial S_1}{\partial t} + (\boldsymbol{q} \cdot \nabla) S_1 = \tau_1 \nabla^2 S_1, \tag{4}$$

$$\frac{\partial S_2}{\partial t} + (\boldsymbol{q} \cdot \nabla) S_2 = \tau_2 \nabla^2 S_2, \tag{5}$$

where $\boldsymbol{q} = (u, v, w)$ is the velocity, p is the pressure, $R_{\mathrm{T}} = \alpha_{\mathrm{T}} g \Delta T K d/(\nu \kappa_{\mathrm{T}})$ is the thermal Darcy-Rayleigh number, $R_{\mathrm{S}i} = \alpha_{\mathrm{S}i} g \Delta S_i K d/(\nu \kappa_{\mathrm{T}})$ $(i = 1, 2)$ is the solute Darcy-Rayleigh number of the ith component, $\Lambda_1 = \lambda_1 \kappa_{\mathrm{T}}/(d^2 \varepsilon)$ is the stress relaxation time parameter, $Pr_{\mathrm{D}} = \nu d^2 \varepsilon^2/(\kappa_{\mathrm{T}} K)$ is the Darcy-Prandtl number, $\tau_i = \kappa_{\mathrm{S}i}/\kappa_{\mathrm{T}}$ $(i = 1, 2)$ is the ratio of diffusivities, $A = M/\varepsilon$, in which ε is the porosity, K is the permeability of the porous medium, λ_1 is the relaxation time, M is the ratio of heat capacities, κ_{T} is the thermal diffusivity, κ_{S1} and κ_{S2} are the solute analogs of κ_{T}, α_{T} is the thermal expansion coefficient, and α_{S1} and α_{S2} are the solute analogs of α_{T}. It should be noted that the considered modified Darcy-Maxwell model includes the classical viscous Newtonian fluid, which is taken as a special case for $\Lambda_1 = 0$.

The following transformations are used in non-dimensionalizing the governing equations:

$$\begin{cases} (x, y, z) = d(x^*, y^*, z^*), \quad \boldsymbol{q}^* = \dfrac{\boldsymbol{q} d}{\kappa_{\mathrm{T}}}, \quad p^* = \dfrac{pK}{\mu \kappa_{\mathrm{T}}}, \\ t^* = \dfrac{\kappa_{\mathrm{T}} t}{d^2 \varepsilon}, \quad T^* = \dfrac{T - T_{\mathrm{L}}}{\Delta T}, \quad S_i^* = \dfrac{S_i - S_{i\mathrm{L}}}{\Delta S_i} \ (i = 1, 2). \end{cases} \tag{6}$$

The boundary conditions are

$$\boldsymbol{q} \cdot \widehat{k} = 0 \quad \text{at} \quad z = 0, 1, \tag{7}$$

$$(T, S_1, S_2) = (0, 0, 0) \quad \text{at} \quad z = 0, \tag{8}$$

$$(T, S_1, S_2) = (-1, -1, -1) \quad \text{at} \quad z = 1. \tag{9}$$

The steady basic state is quiescent and considered as follows:

$$\boldsymbol{q}_{\mathrm{b}} = 0, \quad p = p_{\mathrm{b}}(z), \quad T = T_{\mathrm{b}}(z), \quad S_i = S_{i\mathrm{b}}(z) \ (i = 1, 2). \tag{10}$$

The basic state temperature, solute concentration, and pressure distributions are

$$\begin{cases} T_{\mathrm{b}}(z) = -z, \quad S_{i\mathrm{b}}(z) = -z \ (i = 1, 2), \\ p_{\mathrm{b}}(z) = p_0 + (R_{\mathrm{S1}} + R_{\mathrm{S2}} - R_{\mathrm{T}}) z^2/2, \end{cases} \tag{11}$$

where p_0 is the pressure at $z = 0$. Since the temperature and solute concentrations vary linearly with respect to the vertical coordinate z, perturbing the basic state and following the standard stability analysis procedure, we can obtain the following nonlinear stability equations:

$$\mathcal{L} \boldsymbol{\zeta} = (0, J(\psi, T), J(\psi, S_1), J(\psi, S_2))^{\mathrm{T}}, \tag{12}$$

where $\mathcal{L}$ is the linear differential operator given by

$$\mathcal{L} = \begin{pmatrix} \left(\frac{1}{Pr_{\mathrm{D}}} L \dfrac{\partial}{\partial t} + 1\right) \nabla^2 & R_{\mathrm{T}} L \dfrac{\partial}{\partial x} & -R_{\mathrm{S1}} L \dfrac{\partial}{\partial x} & -R_{\mathrm{S2}} L \frac{\partial}{\partial x} \\ \dfrac{\partial}{\partial x} & A \dfrac{\partial}{\partial t} - \nabla^2 & 0 & 0 \\ \dfrac{\partial}{\partial x} & 0 & \dfrac{\partial}{\partial t} - \tau_1 \nabla^2 & 0 \\ \dfrac{\partial}{\partial x} & 0 & 0 & \dfrac{\partial}{\partial t} - \tau_2 \nabla^2 \end{pmatrix},$$

$\boldsymbol{\zeta} = (\psi, T, S_1, S_2)^{\mathrm{T}}$, $J(\cdot,\cdot)$ stands for the Jacobian with respect to x and z, $\psi(x,z,t)$ is the stream function, $L = \left(1 + \Lambda_1 \frac{\partial}{\partial t}\right)$, and $\nabla^2 = \frac{\partial^2}{\partial x^2} + \frac{\partial^2}{\partial z^2}$ is the Laplacian operator.

The boundary conditions now become

$$\psi = T = S_1 = S_2 = 0 \quad \text{at} \quad z = 0, 1. \tag{13}$$

3 Weakly nonlinear stability analysis

A weakly nonlinear stability analysis is carried out to analyze the stability of the bifurcating periodic solution with the perturbation method. Accordingly, the dependent variables ψ, T, S_1, and S_2 and the thermal Darcy-Rayleigh number R_{T} are expanded in power series of a small perturbation parameter χ ($\ll 1$)[37–38] as follows:

$$\begin{cases} R_{\mathrm{T}} = R_{\mathrm{T}1} + \chi^2 R_{\mathrm{T}2} + \cdots, \quad \psi = \displaystyle\sum_{n=1}^{\infty} \psi_n \chi^n, \\ T = \displaystyle\sum_{n=1}^{\infty} T_n \chi^n, \quad S_1 = \displaystyle\sum_{n=1}^{\infty} S_{1n} \chi^n, \quad S_2 = \displaystyle\sum_{n=1}^{\infty} S_{2n} \chi^n, \end{cases} \tag{14}$$

while the other parameters Pr_{D}, A, Λ_1, τ_1, τ_2, $R_{\mathrm{S}1}$, and $R_{\mathrm{S}2}$ are taken as given. At each stage in the expansion, a column vector may be defined by

$$\boldsymbol{\zeta}_n = (\psi_n, T_n, S_{1n}, S_{2n})^{\mathrm{T}} \ (n = 1, 2, 3, \cdots).$$

The scaling for the time variable t is allowed such that

$$\frac{\partial}{\partial t} = \frac{\partial}{\partial t} + \chi^2 \frac{\partial}{\partial s}.$$

In Eq. (14), $R_{\mathrm{T}1}$ is of no significance because it becomes zero due to the symmetry when the solvability condition is imposed. Substituting Eq. (14) into Eq. (12) and equating like powers of χ yield a series of linear partial differential equations at each order.

3.1 First-order system: linear instability analysis

At the leading order in χ, the equations are linear and homogeneous. Therefore, the first-order problem reduces to the linear instability problem for overstability, and we have

$$\mathcal{L}\boldsymbol{\zeta}_{\mathbf{1}} = 0. \tag{15}$$

The solution of Eq. (15) satisfying the boundary conditions is assumed as follows:

$$\psi_1 = (A_1 \mathrm{e}^{\mathrm{i}\omega t} + \overline{A}_1 \mathrm{e}^{-\mathrm{i}\omega t}) \sin(\alpha x) \sin(\pi z), \tag{16}$$

$$T_1 = (B_1 \mathrm{e}^{\mathrm{i}\omega t} + \overline{B}_1 \mathrm{e}^{-\mathrm{i}\omega t}) \cos(\alpha x) \sin(\pi z), \tag{17}$$

$$S_{11} = (C_1 \mathrm{e}^{\mathrm{i}\omega t} + \overline{C}_1 \mathrm{e}^{-\mathrm{i}\omega t}) \cos(\alpha x) \sin(\pi z), \tag{18}$$

$$S_{21} = (D_1 \mathrm{e}^{\mathrm{i}\omega t} + \overline{D}_1 \mathrm{e}^{-\mathrm{i}\omega t}) \cos(\alpha x) \sin(\pi z), \tag{19}$$

where the overbar denotes the complex conjugate. The amplitudes $(A_1 - D_1)$ and $(\overline{A}_1 - \overline{D}_1)$ are allowed to vary over the slow time s. The relation between the amplitudes is obtained by substituting Eqs. (16)–(19) into Eq. (15) as follows:

$$A_1 = -\frac{(\delta^2 + \mathrm{i}\omega A)}{\alpha} B_1, \quad C_1 = \frac{(\delta^2 + \mathrm{i}\omega A)}{(\delta^2 \tau_1 + \mathrm{i}\omega)} B_1, \quad D_1 = \frac{(\delta^2 + \mathrm{i}\omega A)}{(\delta^2 \tau_2 + \mathrm{i}\omega)} B_1, \tag{20}$$

where $\delta^2 = \alpha^2 + \pi^2$. The amplitude B_1 remains to be undetermined at this stage, and it will be determined from the solvability condition of the $O(\chi^3)$ equation. In Eq. (15), the first equation gives an expression for the thermal Darcy-Rayleigh number for the occurrence of oscillatory convection, and this can be written (after clearing the complex quantities from the denominator) as follows:

$$R_{\mathrm{T}} = \frac{\tau_1\delta^4 + A\omega^2}{\omega^2 + \tau_1^2\delta^4} R_{\mathrm{S1}} + \frac{\tau_2\delta^4 + A\omega^2}{\omega^2 + \tau_2^2\delta^4} R_{\mathrm{S2}} + \frac{\delta^4}{\alpha^2}\Big(\frac{1}{1+\omega^2\Lambda_1^2}\Big) + \frac{A\omega^2\delta^2}{\alpha^2}\Big(\frac{\Lambda_1}{1+\omega^2\Lambda_1^2} - \frac{1}{Pr_{\mathrm{D}}}\Big), \tag{21}$$

and ω^2 satisfies

$$a_1(\omega^2)^3 + a_2(\omega^2)^2 + a_3(\omega^2) + a_4 = 0, \tag{22}$$

where

$$\begin{cases} a_1 = \delta^2\Lambda_1^2, \\ a_2 = \alpha^2 Pr_{\mathrm{D}}\varphi_1\Lambda_1^2 R_{\mathrm{S1}} + \alpha^2 Pr_{\mathrm{D}}\varphi_2\Lambda_1^2 R_{\mathrm{S2}} - Pr_{\mathrm{D}}\delta^2\Lambda_1 + \delta^2 + \tau\Lambda_1^2\delta^6 + APr_{\mathrm{D}}, \\ a_3 = \alpha^2 Pr_{\mathrm{D}}\varphi_1(1+\Lambda_1^2\tau_2^2\delta^4)R_{\mathrm{S1}} + \alpha^2 Pr_{\mathrm{D}}\varphi_2(1+\Lambda_1^2\tau_1^2\delta^4)R_{\mathrm{S2}} - Pr_{\mathrm{D}}\delta^6\Lambda_1\tau + \tau\delta^6 \\ \qquad + \Lambda_1^2\tau_1^2\tau_2^2\delta^{10} + APr_{\mathrm{D}}\tau\delta^4, \\ a_4 = \alpha^2 Pr_{\mathrm{D}}\varphi_1\tau_2^2\delta^4 R_{\mathrm{S1}} + \alpha^2 Pr_{\mathrm{D}}\varphi_2\tau_1^2\delta^4 R_{\mathrm{S2}} - Pr_{\mathrm{D}}\delta^{10}\Lambda_1\tau_1^2\tau_2^2 + \tau_1^2\tau_2^2\delta^{10} + APr_{\mathrm{D}}\tau_1^2\tau_2^2\delta^8. \end{cases}$$

In the above equations,

$$\tau = \tau_1^2 + \tau_2^2, \quad \varphi_i = A\tau_i - 1 \ (i = 1, 2).$$

Equation (22) shows that, for a suitable combination of the dimensionless parameters Pr_{D}, A, Λ_1, τ_1, τ_2, R_{S1}, and R_{S2}, it is possible to have either two or three different real positive values of ω^2 at the same wave number α. In that case, for each one of these frequency values ($\omega^2 > 0$), there is a corresponding real value of the thermal Darcy-Rayleigh number on the oscillatory neutral curve.

For a singly diffusive case ($R_{\mathrm{S1}} = R_{\mathrm{S2}} = 0$), it is observed that oscillatory convection occurs, i.e.,

$$\omega^2 = \frac{\delta^2 Pr_{\mathrm{D}}\Lambda_1 - \delta^2 - APr_{\mathrm{D}}}{\delta^2\Lambda_1^2} > 0. \tag{23}$$

Thus, the necessary condition for the occurrence of oscillatory convection is

$$\Lambda_1 > \frac{1}{Pr_{\mathrm{D}}} + \frac{A}{\delta^2}. \tag{24}$$

For a doubly diffusive case (e.g., $R_{\mathrm{S2}} = 0$), we obtain a dispersion relation quadratic in ω^2 as follows:

$$b_1(\omega^2)^2 + b_2(\omega^2) + b_3 = 0, \tag{25}$$

where

$$\begin{cases} b_1 = \Lambda_1^2\delta^2, \\ b_2 = \varphi_1 Pr_{\mathrm{D}}\alpha^2\Lambda_1^2 R_{\mathrm{S1}} - \Lambda_1\delta^2 Pr_{\mathrm{D}} + (1+\tau_1^2\Lambda_1^2\delta^4)\delta^2 + APr_{\mathrm{D}}, \\ b_3 = \varphi_1 Pr_{\mathrm{D}}\alpha^2 R_{\mathrm{S1}} - \Lambda_1\tau_1^2\delta^6 Pr_{\mathrm{D}} + \tau_1^2\delta^6 + \tau_1^2\delta^4 APr_{\mathrm{D}}. \end{cases}$$

Since $\omega^2 > 0$ for the occurrence of oscillatory convection, a careful glance at Eq. (25) provides the necessary conditions as follows:

$$\tau_1 < \frac{1}{A}, \quad \Lambda_1 > \frac{1}{Pr_{\mathrm{D}}} + \frac{A}{\delta^2}. \tag{26}$$

The condition $\omega = 0$ corresponds to the stationary onset. Thus,

$$R_{\mathrm{T}}^{\mathrm{S}} = \frac{R_{\mathrm{S}1}}{\tau_1} + \frac{R_{\mathrm{S}2}}{\tau_2} + \frac{(\alpha^2+\pi^2)^2}{\alpha^2} \tag{27}$$

is the thermal Darcy-Rayleigh number, above which the layer is unstable. It is observed that Eq. (27) is independent of the viscoelastic parameter, which indicates that the effect of viscoelasticity appears only in the case of time dependent motion. We note that $R_{\mathrm{T}}^{\mathrm{S}}$ attains its critical value at $\alpha_{\mathrm{c}} = \pi$ and the critical thermal Darcy-Rayleigh number for the stationary onset is

$$R_{\mathrm{T}}^{\mathrm{Sc}} = \frac{R_{\mathrm{S}1}}{\tau_1} + \frac{R_{\mathrm{S}2}}{\tau_2} + 4\pi^2. \tag{28}$$

We can obtain important information about the neutral stability curves in the (α, R_{T})-plane by locating the bifurcation points, at which the steady and oscillatory neutral curves meet. These will occur on the steady neutral curve at the wave number α_{b}, for which $\omega = 0$ is a root of Eq. (22). Thus, $a_4(\alpha_{\mathrm{b}}) = 0$ or equivalently

$$\begin{aligned}&\pi^6\varpi + APr_{\mathrm{D}}\pi^2 + \alpha_{\mathrm{b}}^2\Big(3\pi^4\varpi + 2\pi^2APr_{\mathrm{D}} + \frac{Pr_{\mathrm{D}}\varphi_1\delta^4R_{\mathrm{S}1}}{\tau_1^2} + \frac{Pr_{\mathrm{D}}\varphi_2\delta^4R_{\mathrm{S}2}}{\tau_2^2}\Big)\\ &+ (3\pi^2\varpi + APr_{\mathrm{D}})(\alpha_{\mathrm{b}}^2)^2 + \varpi(\alpha_{\mathrm{b}}^2)^3 = 0,\end{aligned} \tag{29}$$

where $\varpi = 1 - \Lambda_1 Pr_{\mathrm{D}}$. For any chosen parametric values, the critical value of R_{T}^0 with respect to the wave number, which is denoted by R_{Tc}^0, is determined as follows. Equation (22) is solved first to determine the positive values of ω^2. If there are no positive values of ω^2, no oscillatory convection is possible. If there is only one positive value of ω^2, the critical value of R_{T}^0 with respect to the wave number is calculated numerically from Eq. (21). If there are two or more positive values of ω^2, the least of R_{T}^0 amongst these two ω^2 is retained to find the critical value of R_{T}^0 with respect to the wave number.

3.2 Second-order system

At order χ^2, the equation is inhomogeneous and given by

$$\mathcal{L}\boldsymbol{\zeta}_2 = (R_{21}, R_{22}, R_{23}, R_{24})^{\mathrm{T}}, \tag{30}$$

where

$$R_{21} = 0, \quad R_{22} = \frac{\pi\alpha}{2}(B_1\overline{A}_1 + \overline{B}_1A_1 + A_1B_1\mathrm{e}^{2\mathrm{i}\omega t} + \overline{A}_1\overline{B}_1\mathrm{e}^{-2\mathrm{i}\omega t})\sin(2\pi z), \tag{31}$$

$$R_{23} = \frac{\pi\alpha}{2}(C_1\overline{A}_1 + \overline{C}_1A_1 + A_1C_1\mathrm{e}^{2\mathrm{i}\omega t} + \overline{A}_1\overline{C}_1\mathrm{e}^{-2\mathrm{i}\omega t})\sin(2\pi z), \tag{32}$$

$$R_{24} = \frac{\pi\alpha}{2}(D_1\overline{A}_1 + \overline{D}_1A_1 + A_1D_1\mathrm{e}^{2\mathrm{i}\omega t} + \overline{A}_1\overline{D}_1\mathrm{e}^{-2\mathrm{i}\omega t})\sin(2\pi z). \tag{33}$$

The above relations suggest that the stream function, temperature, and solute concentration fields involve the terms of the frequency 2ω, and are independent of the fast time scale t.

Thus, the stream function, temperature, and solute concentration fields at second-order can be articulated as follows:

$$\psi_2 = (\psi_{20} + \psi_{22}\mathrm{e}^{2\mathrm{i}\omega t} + \overline{\psi}_{22}\mathrm{e}^{-2\mathrm{i}\omega t})\sin(2\pi z), \tag{34}$$

$$T_2 = (T_{20} + T_{22}\mathrm{e}^{2\mathrm{i}\omega t} + \overline{T}_{22}\mathrm{e}^{-2\mathrm{i}\omega t})\sin(2\pi z), \tag{35}$$

$$S_{12} = (S_{120} + S_{122}\mathrm{e}^{2\mathrm{i}\omega t} + \overline{S}_{122}\mathrm{e}^{-2\mathrm{i}\omega t})\sin(2\pi z), \tag{36}$$

$$S_{22} = (S_{220} + S_{222}\mathrm{e}^{2\mathrm{i}\omega t} + \overline{S}_{222}\mathrm{e}^{-2\mathrm{i}\omega t})\sin(2\pi z), \tag{37}$$

where (ψ_{20}, ψ_{22}), (T_{20}, T_{22}), and $(S_{120}, S_{122}, S_{220}, S_{222})$ are, respectively, the stream function, temperature, and solute concentration fields, and they are independent of the fast time scale. The coefficients ψ_{20}, ψ_{22}, T_{20}, T_{22}, S_{120}, S_{122}, S_{220}, and S_{222} are related to the amplitude at order χ as follows:

$$\begin{cases} T_{20} = \dfrac{\alpha}{8\pi}(A_1\overline{B}_1 + \overline{A}_1 B_1), \quad S_{120} = \dfrac{\alpha}{8\pi\tau_1}(A_1\overline{C}_1 + \overline{A}_1 C_1), \\ S_{220} = \dfrac{\alpha}{8\pi\tau_2}(A_1\overline{D}_1 + \overline{A}_1 D_1), \quad \psi_{20} = 0, \quad T_{22} = \dfrac{\pi\alpha A_1 B_1}{(8\pi^2 + 4\mathrm{i}A\omega)}, \\ S_{122} = \dfrac{\pi\alpha A_1 C_1}{(8\pi^2\tau_1 + 4\mathrm{i}\omega)}, \quad S_{222} = \dfrac{\pi\alpha A_1 D_1}{(8\pi^2\tau_2 + 4\mathrm{i}\omega)}, \quad \psi_{22} = 0. \end{cases} \tag{38}$$

Therefore, the solution at this order is

$$\boldsymbol{\zeta}_2 = (\psi_2, T_2, S_{12}, S_{22})^{\mathrm{T}}. \tag{39}$$

3.3 Third-order system

Now, the equation at order χ^3 is

$$\mathcal{L}\boldsymbol{\zeta}_3 = (R_{31}, R_{32}, R_{33}, R_{34})^{\mathrm{T}}, \tag{40}$$

where

$$\begin{aligned} R_{31} = &-\frac{1}{Pr_{\mathrm{D}}}\frac{\partial}{\partial s}\Big(L + \Lambda_1\frac{\partial}{\partial t}\Big)\nabla^2\psi_1 - R_{\mathrm{T}2}L\frac{\partial T_1}{\partial x} \\ &- \Lambda_1\frac{\partial^2}{\partial x\partial s}(R_{\mathrm{Tc}}^0 T_1 - R_{\mathrm{S}1}S_{11} - R_{\mathrm{S}2}S_{21}), \end{aligned} \tag{41}$$

$$R_{32} = -A\frac{\partial T_1}{\partial s} + J(\psi_1, T_2), \tag{42}$$

$$R_{33} = -\frac{\partial S_{11}}{\partial s} + J(\psi_1, S_{12}), \tag{43}$$

$$R_{34} = -\frac{\partial S_{21}}{\partial s} + J(\psi_1, S_{22}). \tag{44}$$

The third-order equations have the solution as follows:

$$\psi_3 = A_3\mathrm{e}^{\mathrm{i}\omega t}\sin(\alpha x)\sin(\pi z) + \cdots, \tag{45}$$

$$T_3 = B_3\mathrm{e}^{\mathrm{i}\omega t}\cos(\alpha x)\sin(\pi z) + \cdots, \tag{46}$$

$$S_{13} = C_3\mathrm{e}^{\mathrm{i}\omega t}\cos(\alpha x)\sin(\pi z) + \cdots, \tag{47}$$

$$S_{23} = D_3\mathrm{e}^{\mathrm{i}\omega t}\cos(\alpha x)\sin(\pi z) + \cdots. \tag{48}$$

The right-hand-side terms of Eq. (40) have been evaluated from the previously known solutions at orders χ and χ^2. The algebra involved in finding the solutions at this order is straightforward. Therefore, only the results are presented here. We derive the solvability condition for Eq. (40), which is in the form of a first-order nonlinear ordinary differential equation (cubic Landau equation) for the unknown complex amplitude B_1 as follows:

$$\gamma\frac{\mathrm{d}B_1}{\mathrm{d}s}=\Big(\frac{\alpha^2}{\delta^2}(1+\mathrm{i}\omega\Lambda_1)\Delta_1 R_{\mathrm{T2}}-\eta B_1\overline{B}_1\Big)B_1, \tag{49}$$

where

$$\begin{aligned}\gamma=\;&A-\frac{\alpha^2\Lambda_1\Delta_1}{\delta^2}R_{\mathrm{Tc}}^{o}+\frac{\Delta_1(1+2\mathrm{i}\omega\Lambda_1)(\delta^2+\mathrm{i}\omega A)}{Pr_{\mathrm{D}}}\\&-\Big(\frac{\alpha^2\Delta_1(1+\mathrm{i}\omega\Lambda_1)}{\delta^2(\tau_1\delta^2+\mathrm{i}\omega)^2}R_{\mathrm{S1}}+\frac{\alpha^2\Delta_1(1+\mathrm{i}\omega\Lambda_1)}{\delta^2(\tau_2\delta^2+\mathrm{i}\omega)^2}R_{\mathrm{S2}}-\frac{\alpha^2\Delta_1\Lambda_1}{\delta^2(\tau_1\delta^2+\mathrm{i}\omega)}R_{\mathrm{S1}}\Big)(\delta^2+\mathrm{i}\omega A)\\&+\frac{\alpha^2\Delta_1\Lambda_1}{\delta^2}\frac{(\delta^2+\mathrm{i}\omega A)}{(\tau_2\delta^2+\mathrm{i}\omega)}R_{\mathrm{S2}}+\frac{\alpha^2A\Delta_1}{\delta^2}\frac{(1+\mathrm{i}\omega\Lambda_1)}{(\tau_1\delta^2+\mathrm{i}\omega)}R_{\mathrm{S1}}+\frac{\alpha^2A\Delta_1}{\delta^2}\frac{(1+\mathrm{i}\omega\Lambda_1)}{(\tau_2\delta^2+\mathrm{i}\omega)}R_{\mathrm{S2}},\end{aligned} \tag{50}$$

$$\begin{aligned}\eta=\;&\frac{\alpha^2\Delta_1}{\delta^2}\frac{(1+\mathrm{i}\omega\Lambda_1)(\delta^2+\mathrm{i}\omega A)}{(\tau_1\delta^2+i\omega)}\Big(\Delta_2-\frac{(\delta^4+\omega^2A^2)(3\pi^2\delta^2\tau_1+\mathrm{i}\omega(\delta^2-\pi^2))}{4(\tau_1^2\delta^4+\omega^2)(2\pi^2\tau_1+\mathrm{i}\omega)}\Big)R_{\mathrm{S1}}\\&+\frac{\alpha^2\Delta_1}{\delta^2}\frac{(1+\mathrm{i}\omega\Lambda_1)(\delta^2+\mathrm{i}\omega A)}{(\tau_2\delta^2+\mathrm{i}\omega)}\Big(\Delta_2-\frac{(\delta^4+\omega^2A^2)(3\pi^2\delta^2\tau_2+\mathrm{i}\omega(\delta^2-\pi^2))}{4(\tau_2^2\delta^4+\omega^2)(2\pi^2\tau_2+\mathrm{i}\omega)}\Big)R_{\mathrm{S2}}\\&+(\delta^2+\mathrm{i}\omega A)\Delta_2.\end{aligned} \tag{51}$$

In the above equations,

$$\Delta_1=\frac{Pr_{\mathrm{D}}}{Pr_{\mathrm{D}}+\mathrm{i}\omega(1+\mathrm{i}\omega\Lambda_1)},\quad \Delta_2=\frac{3\pi^2\delta^2+\mathrm{i}\omega A(\delta^2+\pi^2)}{8\pi^2+4\mathrm{i}\omega A}.$$

Let B_1 in the phase-amplitude form be as follows:

$$B_1=|B_1|\mathrm{e}^{\mathrm{i}\theta}. \tag{52}$$

Let

$$\Big(\frac{\alpha^2}{\delta^2}(1+\mathrm{i}\omega\Lambda_1)\Big)\Delta_1\gamma^{-1}=\beta_r+\mathrm{i}\beta_i,\quad \gamma^{-1}\eta=\xi_r+\mathrm{i}\xi_i.$$

Then, substituting the above equations into Eq. (49) yields

$$\frac{\mathrm{d}|B_1|^2}{\mathrm{d}s}=2R_{\mathrm{T2}}\beta_r|B_1|^2-2\xi_r|B_1|^4, \tag{53}$$

$$\frac{\mathrm{d}(ph(B_1))}{\mathrm{d}s}=R_{\mathrm{T2}}\beta_i-\xi_i|B_1|^2, \tag{54}$$

where $ph(\cdot)$ represents the phase shift. The magnitude and direction of the periodic convective solution and also the frequency shift are determined in Eq. (49). The nature of bifurcation depends on the sign of the quantity as follows:

$$\Omega=\frac{\beta_r}{\xi_r}. \tag{55}$$

If $\Omega > 0$, the bifurcation is supercritical and stable. If $\Omega < 0$, the bifurcation is subcritical and unstable. The temporal evolution of $|B_1|$ can be expressed as a function of the initial amplitude B_0[39] as follows:

$$|B_1|^2 = \frac{B_0^2}{(\xi_r/(R_{\mathrm{T2}}\beta_r))B_0^2 + (1 - (\xi_r/(R_{\mathrm{T2}}\beta_r))B_0^2)\exp(-2R_{\mathrm{T2}}\beta_r s)}. \tag{56}$$

From the above equation, it follows that $|B_1| \sim B_0 \exp(R_{\mathrm{T2}}\beta_r s)$ when $s \to -\infty$ and $|B_1| \to 0$, which is just as the linear theory. However, $|B_1| \to \sqrt{R_{\mathrm{T2}}\beta_r/\xi_r}$ when $s \to \infty$, which is independent of the value of B_0.

4 Heat and mass transfer

The time and area-averaged thermal Nusselt number ($\overline{Nu}_{\mathrm{T}}$) and the solute Nusselt numbers ($\overline{Nu}_{\mathrm{S1}}, \overline{Nu}_{\mathrm{S2}}$) are determined[23] as follows:

$$\overline{Nu}_{\mathrm{T}} = 1 + \frac{\delta^2}{2}\Omega(R_{\mathrm{T}} - R_{\mathrm{Tc}}^0), \tag{57}$$

$$\overline{Nu}_{\mathrm{S1}} = 1 + \frac{\delta^2(\delta^4 + \omega^2 A^2)}{2(\delta^4\tau_1^2 + \omega^2)}\Omega(R_{\mathrm{T}} - R_{\mathrm{Tc}}^0), \tag{58}$$

$$\overline{Nu}_{\mathrm{S2}} = 1 + \frac{\delta^2(\delta^4 + \omega^2 A^2)}{2(\delta^4\tau_2^2 + \omega^2)}\Omega(R_{\mathrm{T}} - R_{\mathrm{Tc}}^0). \tag{59}$$

5 Results and discussion

The triple diffusive convection in a layer of Maxwell fluid-saturated porous media has been investigated by performing both linear instability and weakly nonlinear stability analyses. The linear instability analysis has revealed some interesting results under certain conditions, which has not been observed hitherto in the literature. This has been achieved through a systematic study on the topology of neutral stability curves. Based on the weakly nonlinear stability analysis, a cubic Landau equation is derived, and the stability of the oscillatory bifurcating solution is analyzed. The heat and mass transfer is quantified in terms of the Nusselt numbers.

The neutral stability curves in the (α, R_{T}) plane are illustrated in Figs. 2 and 3 for different values of the stress relaxation parameter Λ_1, Darcy-Prandtl number Pr_{D}, and solute Darcy-Rayleigh number R_{S1} for the chosen parametric values. These figures show that the

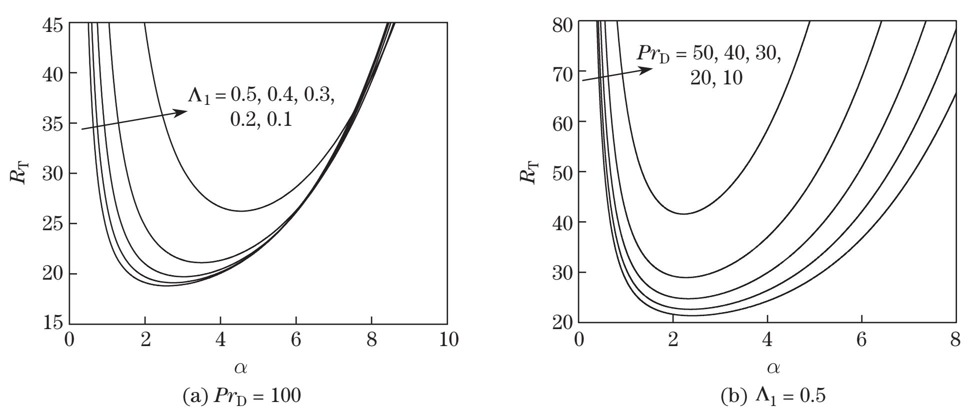

Fig. 2 Oscillatory neutral stability curves in the (α, R_{T}) plane for different values of Λ_1 and Pr_{D} when $A = 1$, $\tau_1 = 0.2$, $\tau_2 = 0.27$, $R_{\mathrm{S1}} = -30$, and $R_{\mathrm{S2}} = 80$

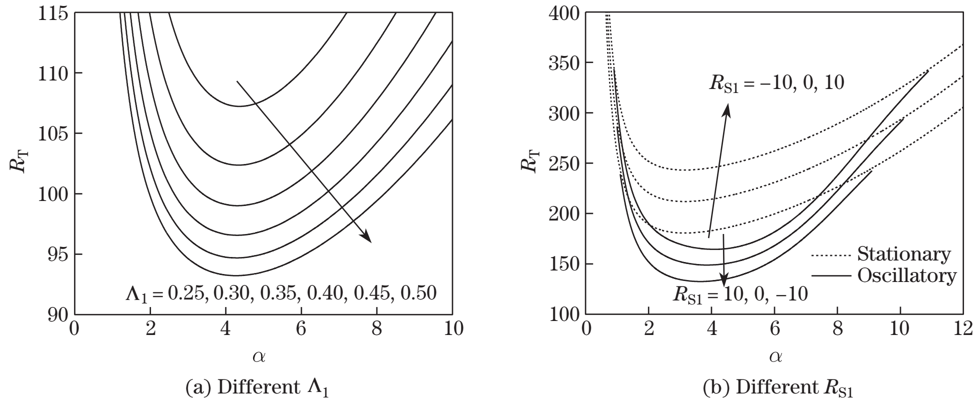

Fig. 3 Neutral stability curves in the $(\alpha, R_{\rm T})$ plane for different values of (a) Λ_1 when $Pr_{\rm D} = 10$, $A = 1.2$, $\tau_1 = 1.0$, $\tau_2 = 1.1$, $R_{\rm S1} = -10$, and $R_{\rm S2} = 100$ and (b) $R_{\rm S1}$ when $Pr_{\rm D} = 20$, $\Lambda_1 = 0.05$, $A = 2$, $\tau_1 = 0.32$, $\tau_2 = 0.29$, and $R_{\rm S2} = 50$

stationary and oscillatory neutral curves are connected in a topological sense, which implies the requirement of single critical thermal Darcy-Rayleigh number to recognize the instability characteristics of the system. Moreover, the increases in Λ_1 (see Figs. 2(a) and 3(a)) and $Pr_{\rm D}$ (Fig. 2(b)) will decrease in the stability region. The stability region gets enlarged with an increase in the positive (i.e., stabilizing) values of $R_{\rm S1}$, while an opposite trend can be seen with an increase in the negative values of $R_{\rm S1}$ (see Fig. 3(b)).

The evolution of the neutral stability curves is displayed in Figs. 4(a)–4(f) for $Pr_{\rm D} = 10$, $A = 2$, $\Lambda_1 = 0.1$, $\tau_1 = 0.159$, $\tau_2 = 0.270$, and $R_{\rm S1} = -15.92$ for positive values of $R_{\rm S2}$ varying from 63 to 59.3. These figures exhibit an altogether different behavior, which indicates significant ramifications on the linear instability of the system. It is seen that the oscillatory neutral curve is connected to the stationary neutral curve at two bifurcation points when $R_{\rm S2} = 63$ (see Fig. 4(a)). The oscillatory neutral curve is skewed slightly towards the lower wave number region, and also pinched on both sides, which gives rise to two values of $R_{\rm T}^0$ for some wave numbers. The upper maximum values of the oscillatory neutral curve lie on top of the minimum value of the stationary neutral curve. The bifurcation points move closer together when $R_{\rm S2}$ is decreased to 61 (see Fig. 4(b)) and starts detaching from the stationary neutral curve when $R_{\rm S2}$ is decreased further to 60 (see Fig. 4(c)). Till this stage, the linear instability of the system can be easily determined by a single value of $R_{\rm T}$. With a further decrease in the value of $R_{\rm S2}$, the closed convex oscillatory neutral curve totally detaches from the stationary curve (see Fig. 4(d)), and moves well below the minimum of the stationary neutral curve (see Fig. 4(e)) when $R_{\rm S2} = 59.5$. The importance of this type of detached oscillatory neutral curves is that it is necessary to have three critical values of $R_{\rm T}$ to specify the linear instability criteria of the Maxwell fluid-saturated porous layer instead of the usual single value. From Fig. 4(e), it is seen that the linear instability criteria involve three values of $R_{\rm T}$, and may be viewed as follows. When $R_{\rm T} < R_{\rm T1}$ and $R_{\rm T2} < R_{\rm T} < R_{\rm T3}$, the layer is linearly stable. When $R_{\rm T1} < R_{\rm T} < R_{\rm T2}$ and $R_{\rm T} > R_{\rm T3}$, the layer is unstable. A further decrease in the value of $R_{\rm S2}$ shows that the closed oscillatory neutral curve collapses to a point and ultimately disappears, which leaves only the stationary neutral curve when $R_{\rm S2} = 59.3$. Nonetheless, one salient feature that does not carry over from the case of Newtonian fluids is the absence of the heart-shaped oscillatory neutral curve within the maxima at the same thermal Darcy-Rayleigh number and different wave numbers.

Figures 5 and 6 exemplify the stability boundaries for the same parametric values considered in Fig. 4. From Fig. 5, we can see that the stability boundary can be viewed individually in three regions. To the right of the point of (A) ($R_{\rm S2} > 60.133\,7$), oscillatory instability first

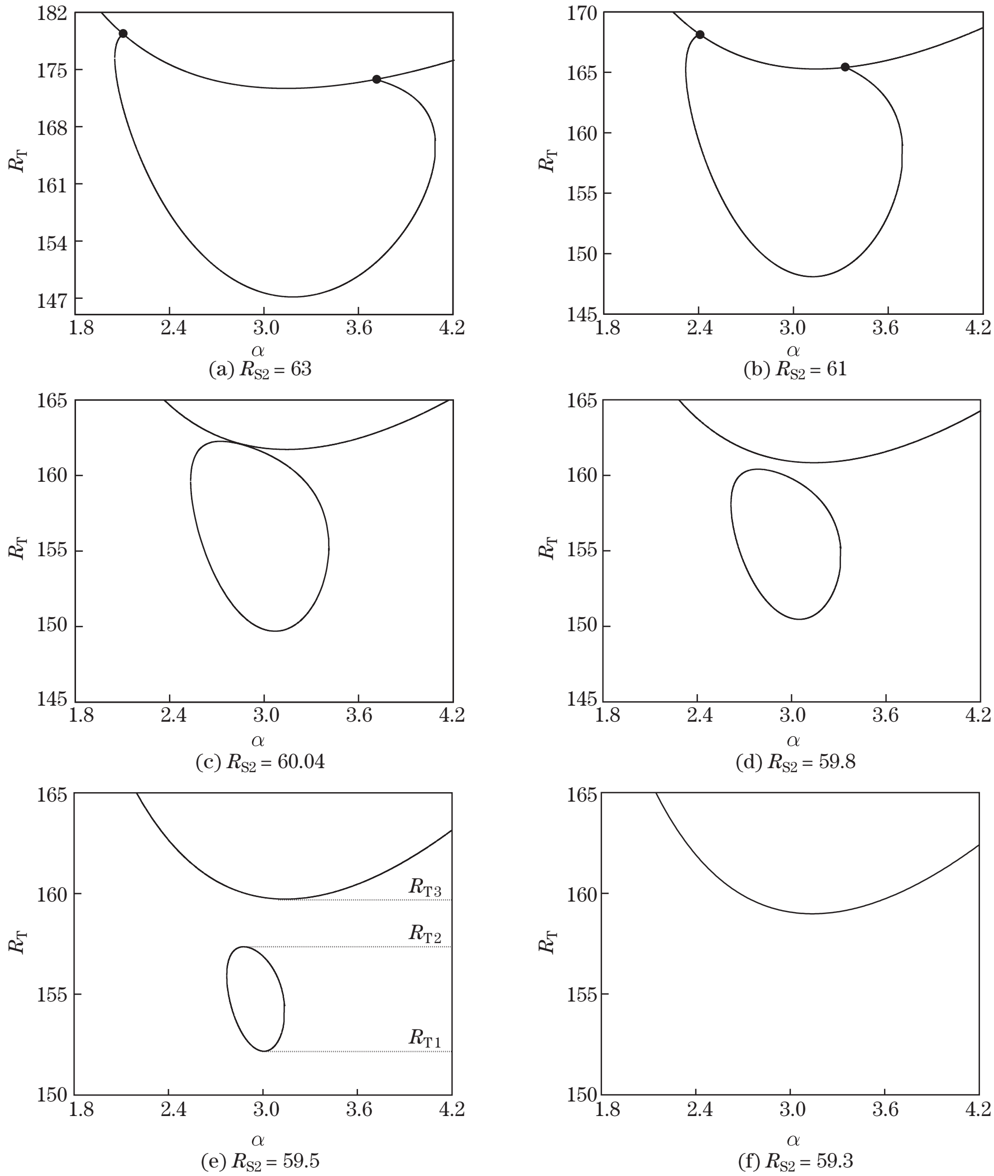

Fig. 4 Evolution of neutral stability curves with $Pr_D = 10$, $A = 2$, $\Lambda_1 = 0.1$, $\tau_1 = 0.159$, $\tau_2 = 0.270$, $R_{S1} = -15.92$, and different R_{S2}

occurs at a lower value of R_T, then stationary instability occurs, and there is a critical thermal Darcy-Rayleigh number R_{Tc}. To the left of the cusp (B) ($R_{S2} < 59.390\,8$), instability occurs as stationary convection, oscillatory instability does not occur, and again there is one value of R_{Tc}. The enlarged version of the figure clearly reveals three distinct regions of R_{S2}, and it is seen that, in some range of R_{S2}, three values of R_{Tc} are needed to specify the linear instability criteria.

The sensitivity of the viscoelastic parameter Λ_1 on disconnected oscillatory neutral curves is elucidated in Figs. 7(a) and 7(b). Although Fig. 7(a) makes obviously the requirement of three values of R_{Tc} to specify the linear instability of the system, a slight deviation in the value of

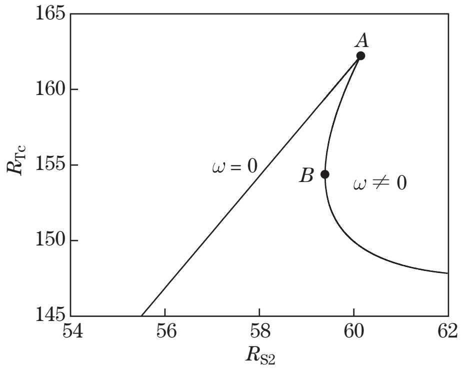

Fig. 5 Stability boundary for $Pr_{\mathrm{D}} = 10$, $A = 2$, $\Lambda_1 = 0.1$, $\tau_1 = 0.159$, $\tau_2 = 0.270$, and $R_{\mathrm{S1}} = -15.92$

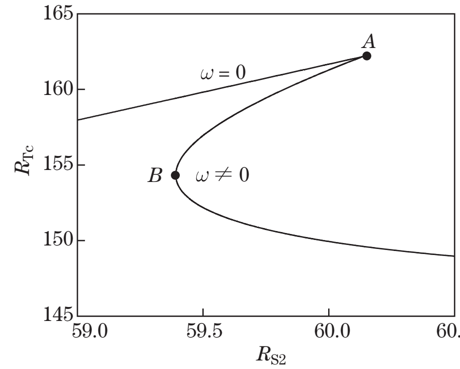

Fig. 6 Expanded view of the multivalued region

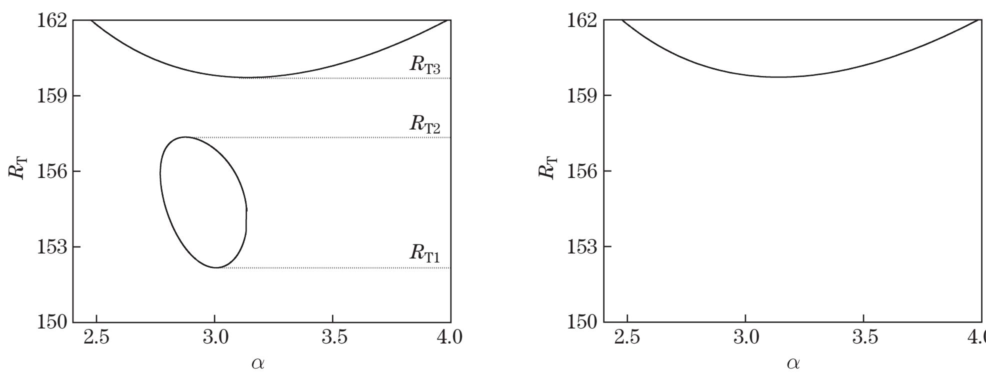

(a) $\Lambda_1 = 0.1$ (b) $\Lambda_1 = 0.099\,3$

Fig. 7 Variations of the relaxation parameter Λ_1 on the evolution of neutral stability curves, where $Pr_{\mathrm{D}} = 10$, $A = 2$, $\tau_1 = 0.159$, $\tau_2 = 0.270$, $R_{\mathrm{S1}} = -15.92$, and $R_{\mathrm{S2}} = 59.5$

Λ_1 (see Fig. 7(b)) entirely changes the instability mode. That is, the instability ceases to be oscillatory and the convective onset turns out to be stationary, which represents the sufficiency of single value of R_{Tc} to specify the linear instability criteria. Thus, the viscoelastic property of the fluid significantly affects the instability characteristics of the system.

It is possible to estimate the parameter set for the boundary separating stationary and oscillatory solutions. This behavior is illustrated in Fig. 8 on a (Pr_{D}, Λ_1) plane for different values of R_{S2} obtained from Eqs. (21) and (28). It is seen that, for fixed values of Pr_{D} and R_{S2}, there exists a value of $\Lambda_1 = \Lambda_1^*$, where $R_{\mathrm{Tc}}^0 = R_{\mathrm{Tc}}^{\mathrm{S}}$. The value of Λ_1^* decreases with the increases in Pr_{D} and R_{S2}. In other words, the critical thermal Darcy-Rayleigh number for the onset of both stationary and oscillatory convection coincides at well-defined parametric values. Therefore, a codimension-two bifurcation occurs. The figure also indicates that the value of the stress relaxation parameter, which represents the crossover between stationary and oscillatory bifurcations, decreases with the increase in the Darcy-Prandtl number. Moreover, the oscillatory region increases with the increase in R_{S2}, which indicates that the presence of the stronger concentration gradient is to support the oscillatory convection as the preferred instability mode.

By use of a weakly nonlinear stability analysis, a cubic Landau equation is derived, and the stability of the oscillatory bifurcating solution is analyzed, which powerfully depends on

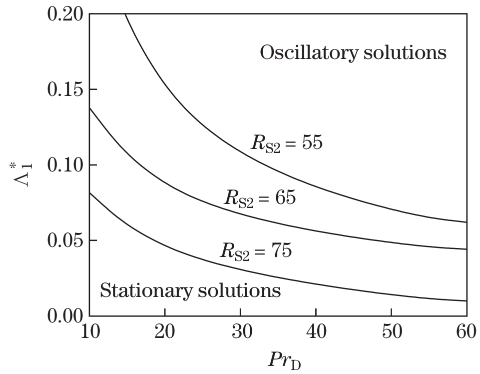

Fig. 8 Stress relaxation parameter Λ_1^* for different values of R_{S2} when $A = 2$, $\tau_1 = 0.15$, $\tau_2 = 0.27$, and $R_{S1} = -20$

the viscoelastic parameter. It is observed that subcritical/supercritical bifurcation is possible, which depends on the choice of the physical parameters. Nonetheless, the bifurcating solution is found to be supercritical (stable) in the absence of additional solute concentration fields. The vigor of triple diffusive convection in the Maxwell fluid-saturated porous medium can be understood by heat and mass transfer. This has been achieved by estimating the thermal and solute Nusselt numbers for oscillatory convection. The time and area-averaged thermal Nusselt number ($\overline{Nu}_{\mathrm{T}}$) and solute Nusselt numbers ($\overline{Nu}_{\mathrm{S1}}$ and $\overline{Nu}_{\mathrm{S2}}$) are displayed as a function of R_{T} for different values of Λ_1 and Pr_{D} in Figs. 9(a) and 9(b), respectively. When R_{T} increases, the heat and mass transfer increases. When Λ_1 and Pr_{D} increase, the heat and mass transfer characteristics of oscillatory convection increase. This may be credited to the fact that the increase in Λ_1 is to increase the overstability vibration. Therefore, its effect is to increase the heat and mass transfer.

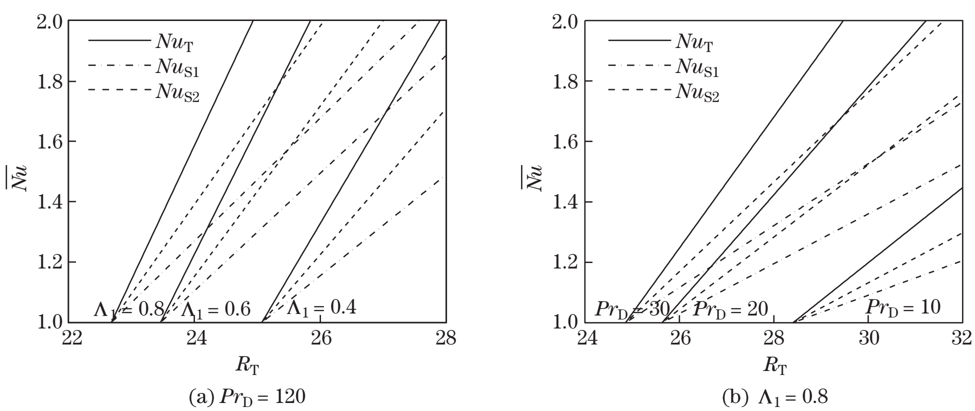

Fig. 9 Nusselt numbers $\overline{Nu}$ ($\overline{Nu}_{\mathrm{T}}, \overline{Nu}_{\mathrm{S1}}, \overline{Nu}_{\mathrm{S2}}$) for different values of Λ_1 and Pr_{D} when $A = 2$, $\tau_1 = 1.5$, $\tau_2 = 1.244$, $R_{\mathrm{S1}} = -20$, and $R_{\mathrm{S2}} = 42$

6 Conclusions

The triple diffusive convection in a Maxwell fluid-saturated porous medium is investigated by use of both linear and weakly nonlinear stability analyses. Moreover, disconnected convex oscillatory neutral curves are found to occur for some choices of the parametric values, which indicates the necessity of three critical thermal Darcy-Rayleigh numbers to specify the linear instability criteria instead of the usual single value. However, it is observed that the instability onset of the motionless basic state cannot occur via the simultaneous passage of two sets of complex conjugate temporal eigenvalues from the left half-plane to the right half-plane at the same critical thermal Darcy-Rayleigh number as observed in the case of Newtonian fluids. The onset of oscillatory convection increases with the increases in the relaxation parameter and the Darcy-Prandtl number. The threshold value of the relaxation parameter, at which codimension-two bifurcation occurs, decreases with the increase in the Darcy-Prandtl number. The stability of the bifurcating oscillatory solution is analyzed by deriving a cubic Landau equation. There is a possibility of bifurcation to be either subcritical (unstable) or supercritical (stable), which depends on the choice of the physical parameters. The variations of the time and area-averaged thermal and solute Nusselt numbers with respect to the thermal Darcy-Rayleigh number are presented. The heat and mass transfer rate increases with the increases in the relaxation parameter and the Darcy-Prandtl number.

Acknowledgements One of the authors (K. R. RAGHUNATHA) wishes to thank the the Department of Science and Technology, New Delhi for granting him a fellowship under the Innovation in Science Pursuit for the Inspired Research (INSPIRE) Program (No. DST/INSPIRE Fellowship/[IF 150253]). The authors wish to thank the reviewers for their helpful suggestions.

References

[1] Nield, D. A. and Bejan, A. *Convection in Porous Media*, Springer International Publishing, Berlin (2017)

[2] Makinde, O. D. and Mhone, P. Y. On temporal stability analysis for hydromagnetic flow in a channel filled with a saturated porous medium. *Flow, Turbulence and Combustion*, **83**, 21–32 (2009)

[3] Makinde, O. D. Thermal stability of a reactive viscous flow through a porous-saturated channel with convective boundary conditions. *Applied Thermal Engineering*, **29**, 1773–1777 (2009)

[4] Makinde, O. D. Magneto-hydromagnetic stability of plane-Poiseuille flow using multi-Deck asymptotic technique. *Mathematical and Computer Modelling*, **37**, 251–259 (2003)

[5] Shenoy, A. V. Non-Newtonian fluid heat transfer in porous media. *Advances in Heat Transfer*, **24**, 101–190 (1994)

[6] Khaled, A. R. A. and Vafai, K. The role of porous media in modeling flow and heat transfer in biological tissues. *International Journal of Heat and Mass Transfer*, **46**, 4989–5003 (2003)

[7] Pascal, H. and Pascal, F. On viscoelastic effects in non-Newtonian steady flows through porous media. *Transport in Porous Media*, **4**, 17–35 (1989)

[8] Pilitsis, S. and Beris, A. N. Calculations of steady-state viscoelastic flow in an undulating tube. *Journal of Non-Newtonian Fluid Mechanics*, **31**, 231–287 (1989)

[9] Rudraiah, N., Kaloni, P. N., and Radhadevi, P. V. Oscillatory convection in a viscoelastic fluid through a porous layer heated from below. *Rheological Acta*, **28**, 48–53 (1989)

[10] Kim, M. C., Lee, S. B., Kim, S., and Chung, B. J. Thermal instability of viscoelastic fluids in porous media. *International Journal of Heat and Mass Transfer*, **46**, 5065–5072 (2003)

[11] Yoon, D. Y., Kim, M. C., and Choi, C. K. The onset of oscillatory convection in a horizontal porous layer saturated with viscoelastic liquid. *Transport in Porous Media*, **55**, 275–284 (2004)

[12] Shivakumara, I. S. and Sureshkumar, S. Convective instabilities in a viscoelastic-fluid-saturated porous medium with through flow. *Journal of Geophysics and Engineering*, **4**, 104–115 (2007)

[13] Shivakumara, I. S., Malashetty, M. S., and Chavaraddi, K. B. Onset of convection in a viscoelastic-fluid-saturated sparsely packed porous layer using a thermal non equilibrium model. *Canadian Journal of Physics*, **84**, 973–990 (2006)

[14] Malashetty, M. S., Shivakumara, I. S., Sridhar, K., and Mahantesh, S. Convective instability of Oldroyd-B fluid saturated porous layer heated from below using a thermal non-equilibrium mode. *Transport in Porous Media*, **64**, 123–139 (2006)

[15] Sheu, L. J., Tam, L. M., Chen, J. H., Chen, H. K., Lin, K. T., and Kang, Y. Chaotic convection of viscoelastic fluids in porous media. *Chaos, Solitons and Fractals*, **37**, 113–124 (2008)

[16] Bertola, V. and Cafaro, E. Thermal instability of viscoelastic fluids in horizontal porous layers as initial problem. *International Journal of Heat and Mass Transfer*, **49**, 4003–4012 (2006)

[17] Sheu, L. J., Chen, J. H., Chen, H. K., Tam, L. M., and Chao, Y. C. A unifed system describing dynamics of chaotic convection. *Chaos*, *Solitons and Fractals*, **41**, 123–130 (2009)

[18] Liu, Y. and Guo, B. Coupling model for unsteady MHD flow of generalized Maxwell fluid with radiation thermal transform. *Applied Mathematics and Mechanics* (*English Edition*), **37**(2), 137–150 (2016) https://doi.org/10.1007/s10483-016-2021-8

[19] Cao, L., Si, X., and Zheng, L. Convection of Maxwell fluid over stretching porous surface with heat source/sink in presence of nanoparticles: Lie group analysis. *Applied Mathematics and Mechanics* (*English Edition*), **37**(4), 433–442 (2016) https://doi.org/10.1007/s10483-016-2052-9

[20] Mahanthesh, B., Gireesha, B. J., Shehzad, S. A., Abbasi, F. M., and Gorla, R. S. R. Nonlinear three-dimensional stretched flow of an Oldroyd-B fluid with convective condition, thermal radiation, and mixed convection. *Applied Mathematics and Mechanics* (*English Edition*), **38**(7), 969–980 (2017) https://doi.org/10.1007/s10483-017-2219-6

[21] Straughan, B. *Stability and Wave Motion in Porous Media*, Springer, New York (2008)

[22] Vafai, K. *Handbook of Porous Media*, Marcel Dekker, New York (2000)

[23] Wang, S. and Tan, W. Stability analysis of soret-driven double-diffusive convection of Maxwell fluid in a porous medium. *International Journal of Heat and Fluid Flow*, **32**, 88–94 (2011)

[24] Malashetty, M. S., Tan, W. C., and Swamy, M. The onset of double diffusive convection in a binary viscoelastic fluid-saturated anisotropic porous layer. *Physics of Fluids*, **21**, 084101–084111 (2009)

[25] Awad, F. G., Sibanda, P., and Motsa, S. S. On the linear stability analysis of a Maxwell fluid with double-diffusive convection. *Applied Mathematical Modelling*, **34**, 3509–3517 (2010)

[26] Griffiths, R. W. The influence of a third diffusing component upon the onset of convection. *Journal of Fluid Mechanics*, **92**, 659–670 (1979)

[27] Pearlstein, A. J., Harris, R. M., and Terrones, G. The onset of convective instability in a triply diffusive of fluid layer. *Journal of Fluid Mechanics*, **202**, 443–465 (1989)

[28] Straughan, B. and Walker, D. W. Multi-component convection-diffusion and penetrative convection. *Fluid Dynamics Research*, **19**, 77–89 (1997)

[29] Straughan, B. and Tracey, J. Multi-component convection-diffusion with internal heating or cooling. *Acta Mechanica*, **133**, 219–239 (1999)

[30] Rudraiah, N. and Vortmeyer, D. Influence of permeability and of a third diffusing component upon the onset of convection in a porous medium. *International Journal of Heat and Mass Transfer*, **25**, 457–464 (1982)

[31] Poulikakos, D. Effect of a third diffusing component on the onset of convection in a horizontal layer. *Physics of Fluids*, **28**, 3172–3174 (1985)

[32] Tracey, J. Multi-component convection-diffusion in a porous medium. *Continuum Mechanics and Thermodynamics*, **8**, 361–381 (1973)

[33] Rionero, S. Long-time behavior of multi-component fluid mixtures in porous media. *International Journal of Engineering Science*, **48**, 1519–1633 (2010)

[34] Rionero, S. Triple diffusive convection in porous media. *Acta Mechanica*, **224**, 447–458 (2013)

[35] Ghalambz, M., Moatter, F., Sheremet, M. A., and Pop, I. Triple-diffusive natural convection in a square porous cavity. *Transport in Porous Media*, **111**, 59–79 (2016)

[36] Zhao, M., Wang, S., and Zhang, Q. Onset of triply diffusive convection in a Maxwell fluid-saturated porous layer. *Applied Mathematical Modelling*, **38**, 2345–2352 (2014)

[37] Venezian, G. Effect of modulation on the onset of thermal convection. *Journal of Fluid Mechanics*, **35**, 243–254 (1969)

[38] Malkus, W. V. R. and Veronis, G. Finite amplitude cellular convection. *Journal of Fluid Mechanics*, **4**, 225–260 (1985)

[39] Drazin, P. G. and Reid, W. H. *Hydrodynamic Stability*, Cambridge University Press, New York (1981)